Human symbionts inject and neutralize antibacterial toxins to persist in the gut

Aaron G. Wexler[a,b], Yiqiao Bao[a,b], John C. Whitney[c], Louis-Marie Bobay[d], Joao B. Xavier[e], Whitman B. Schofield[a,b], Natasha A. Barry[a,b], Alistair B. Russell[c], Bao Q. Tran[f], Young Ah Goo[f], David R. Goodlett[f], Howard Ochman[d], Joseph D. Mougous[c,g], and Andrew L. Goodman[a,b,1]

[a]Department of Microbial Pathogenesis, Yale University School of Medicine, New Haven, CT 06510; [b]Microbial Sciences Institute, Yale University School of Medicine, West Haven, CT 06516; [c]Department of Microbiology, University of Washington School of Medicine, Seattle, WA 98195; [d]Department of Integrative Biology, University of Texas, Austin, TX 78712; [e]Computational Biology Program, Memorial Sloan-Kettering Cancer Center, New York, NY 10065; [f]Department of Pharmaceutical Sciences, School of Pharmacy, University of Maryland, Baltimore, MD 21201; and [g]Howard Hughes Medical Institute, University of Washington School of Medicine, Seattle, WA 98195

Edited by Ralph R. Isberg, Howard Hughes Medical Institute/Tufts University School of Medicine, Boston, MA, and approved February 2, 2016 (received for review December 28, 2015)

The human gut microbiome is a dynamic and densely populated microbial community that can provide important benefits to its host. Cooperation and competition for nutrients among its constituents only partially explain community composition and interpersonal variation. Notably, certain human-associated Bacteroidetes—one of two major phyla in the gut—also encode machinery for contact-dependent interbacterial antagonism, but its impact within gut microbial communities remains unknown. Here we report that prominent human gut symbionts persist in the gut through continuous attack on their immediate neighbors. Our analysis of just one of the hundreds of species in these communities reveals 12 candidate antibacterial effector loci that can exist in 32 combinations. Through the use of secretome studies, in vitro bacterial interaction assays and multiple mouse models, we uncover strain-specific effector/immunity repertoires that can predict interbacterial interactions in vitro and in vivo, and find that some of these strains avoid contact-dependent killing by accumulating immunity genes to effectors that they do not encode. Effector transmission rates in live animals can exceed 1 billion events per minute per gram of colonic contents, and multiphylum communities of human gut commensals can partially protect sensitive strains from these attacks. Together, these results suggest that gut microbes can determine their interactions through direct contact. An understanding of the strategies human gut symbionts have evolved to target other members of this community may provide new approaches for microbiome manipulation.

gut microbiome | microbial ecology | type VI secretion | symbiosis

Interpersonal variation in gut microbial community composition, even at the species or strain level, can determine the contribution of these communities to cancer risk, drug metabolism, caloric extraction from diet, infectious disease resistance, and other responses (1–5). However, the rules that determine community membership, especially at the species or strain level, are largely undefined. The gut environment is characterized by constant peristalsis and extensive niche heterogeneity, and factors previously implicated in shaping these communities (metabolites, vitamins, dietary polysaccharides, host IgA, bacteriocins) are freely diffusible (6–8). In this context, the recent identification of genes encoding type VI secretion systems (T6SSs) in the genomes of many prominent human gut symbionts was unexpected because the ability of these dynamic machines to inject toxic effectors into adjacent cells is strictly dependent on direct cell-to-cell contact (9–12).

The T6SSs of Bacteroidetes share many subunits with those of Proteobacteria; these include the Hcp and TssB–TssC proteins, which interact and assemble into a contractile bacteriophage tail-like structure that is required for effector translocation from donor to recipient cells (9, 10). Bacteria with T6SSs lack a means for self-/non–self-discrimination; thus, sister cells inject one another with effectors. To nullify the antibacterial properties of these toxins, T6SS$^+$ strains produce immunity proteins that directly bind cognate effectors. Despite our growing understanding of the mechanism and activity of T6S in vitro, little is known about the ecological role of this pathway in natural environments where direct encounters between microorganisms occur.

Here we report that the human gut symbiont *Bacteroides fragilis* NCTC 9343 (*B. fragilis*^{N}) targets other members of the microbiome in a species- and strain-specific manner in the mammalian gut. We identify strain-specific effector/immunity (E/I) repertoires and show that the presence or absence of these genes can accurately predict interstrain dynamics in the gut. Furthermore, we combine microbial genetics, mathematical modeling, and gnotobiotic studies to determine the frequency of T6S-mediated events in live animals. Together, these results define a significant role for contact-mediated bacterial antagonism between human gut symbionts.

Results

Human Gut Symbionts Can Target Other Members of the Microbiome in Vivo. The human gut symbiont *B. fragilis*^{N} (13) effectively kills the T6SS$^-$ human gut commensal *Bacteroides thetaiotaomicron* in a T6S-dependent manner in vitro (11). Whether *B. fragilis*^{N} also targets *B. thetaiotaomicron* in the gut is unknown. To test this, we introduced *B. fragilis*^{N} (wild type or a T6S-defective control lacking the gene encoding the T6SS sheath component TssC)

Significance

The microbial community in the human gut represents one of the densest known ecosystems. Community composition has broad impacts on health, and metabolic competition and host selection have both been implicated in shaping these communities. Here, we report that contact-dependent bacterial antagonism also determines the ability of human gut symbionts to persist in the microbiome. Simplified microbiomes, assembled in gnotobiotic mice, reveal effector transmission rates exceeding 1 billion events per minute per gram of colonic contents. Together, these results suggest that human gut symbionts define their closest competitors not only metabolically but also spatially. Moreover, strains within a single species can encode diverse effectors that may provide new avenues for shaping the microbiome to improve human health.

Author contributions: A.G.W. and A.L.G. designed research; A.G.W., Y.B., J.C.W., N.A.B., B.Q.T., and Y.A.G. performed research; A.G.W., L.-M.B., J.B.X., W.B.S., A.B.R., D.R.G., H.O., J.D.M., and A.L.G. analyzed data; and A.G.W. and A.L.G. wrote the paper.

The authors declare no conflict of interest.

This article is a PNAS Direct Submission.

Freely available online through the PNAS open access option.

[1]To whom correspondence should be addressed. Email: andrew.goodman@yale.edu.

This article contains supporting information online at www.pnas.org/lookup/suppl/doi:10.1073/pnas.1525637113/-/DCSupplemental.

and *B. thetaiotaomicron* into germ-free mice by oral gavage, and monitored the abundance of each strain in feces over time. Surprisingly, *B. thetaiotaomicron* colonization was not dependent on *B. fragilis*^{N} T6SS status despite its susceptibility in vitro (Fig. 1 *A* and *B*). By contrast, the T6SS$^-$ human gut symbiont *Bacteroides vulgatus*, which is more closely related to *B. fragilis* based on whole-genome phylogeny (14), shows a moderate but significant degree of susceptibility to *B. fragilis*^{N} T6S attacks in vivo that mirrors its susceptibility in vitro (Fig. 1 *C* and *D*). Together, these data demonstrate that different species within the human microbiome can engage in T6S-dependent antagonism in the mammalian gut, and suggest that certain susceptible species can avoid killing in vivo.

***B. fragilis* Strains Encode Extensive Variation in Effector/Immunity Repertoires.** Based on these results, we reasoned that an important role for T6S in the gut could be to mediate interactions between close evolutionary relatives that share the same niche. We searched draft and complete genomes of all 92 sequenced strains of *B. fragilis* for homologs of eight core T6SS genes (Dataset S1, Tables S1 and S2). Notably, the distribution of T6SS machinery is highly variable within this species: only 60 of the 92 strains encode all eight core genes. Moreover, strain genome phylogeny is not congruent with T6SS core gene phylogeny, indicating limited ancestral inheritance and extensive horizontal gene transfer of T6SS variants across strains (Fig. 2 and Fig. S1). These core genes are located in ∼30-kb islands that are syntenic except for two variable regions (cassette A and cassette B) that encode Hcp proteins, PAAR-containing adaptor proteins, proteins with T6SS effector-like domains, and numerous hypothetical proteins (Fig. 2, *Inset*; Dataset S1, Table S3). Collectively, these *B. fragilis* strains harbor four distinct versions of cassette A and eight distinct versions of cassette B, which could exist in 32 possible combinations. The 60 T6SS-positive strains that have been sequenced represent 24 of these configurations (Fig. 2; Dataset S1, Table S3). Computational analysis of other Bacteroides genomes suggests these features are general (15).

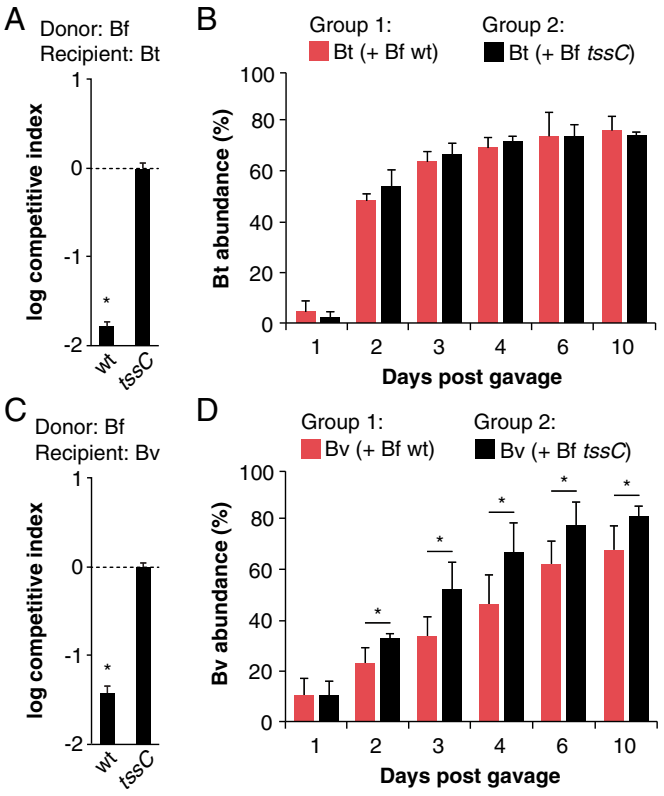

Fig. 1. T6S antagonism in the gut is species-dependent. (*A* and *B*) *B. thetaiotaomicron* (Bt) is susceptible to *B. fragilis*^{N} (Bf) T6S in vitro (*A*) but not in vivo (*B*). (*C* and *D*) *B. vulgatus* (Bv) is susceptible to *B. fragilis*^{N} T6S both in vitro (*C*) and in vivo (*D*). For in vitro competitions (*A* and *C*), competitive index calculations are normalized to *tssC* controls and $*P < 0.05$. Error bars indicate ± SD ($n = 2$; representative of four independent trials). For gnotobiotic mouse studies (*B* and *D*), *B. thetaiotaomicron* or *B. vulgatus* was introduced into germ-free mice with WT (red bars) or *tssC* (black bars) *B. fragilis*^{N}, and the abundance of each strain was determined by quantitative PCR using gDNA from fecal samples collected over time. $*P < 0.05$ between recipient populations in each group ($n = 5$ mice per group; representative of two independent trials); error bars indicate ± SD.

Based on the presence of genes encoding putative effector and adaptor proteins, we hypothesized that these cassettes might encode E/I pairs that mediate cytotoxicity against recipient cells. Indeed, secretome analysis of *B. fragilis*^{N} revealed six proteins that are present specifically in the secretome of the wild-type strain but not the *tssC* control strain (Fig. 3*A*; Dataset S1, Table S4). Three of these proteins are homologs of the secreted proteobacterial T6SS structural proteins Hcp [also observed in a recent study (16)] and VgrG, and the fourth contains a PAAR-repeat domain typical of T6SS adaptors (9, 10). Of the two remaining proteins, BF9343_1937 lacks any known T6S effector domains, and BF9343_1928 contains a MIX domain found in other T6SS effectors (17). These proteins have no previously known function and are encoded, along with the PAAR adaptor, within cassettes A and B of *B. fragilis*^{N} (Fig. 3*A*).

T6S effectors are typically encoded in tandem with their cognate immunity genes (10). To test whether BF9343_1936 and BF9343_1927-6 (homologs) function as immunity genes, we examined the ability of *B. fragilis*^{N} to kill isogenic *tssC* recipient cells missing one or both of these loci. Indeed, deletion of either candidate E/I pair increases recipient sensitivity to killing by wild-type (but not *tssC*) donor cells by orders of magnitude (Fig. 3*B*). In-frame deletion of the candidate E/I pairs from the wild-type strain, and constitutive expression of the candidate immunity genes in a *tssC* recipient strain lacking both E/I pairs, confirmed that each immunity protein confers protection against T6S-mediated cell killing in an effector-specific manner (Fig. 3*C*). Based on these observations, we assigned BF9343_1937 and BF9343_1928 the names *bte1* (*B. fragilis* T6S effector 1) and *bte2*, and the cognate immunity genes BF9343_1936 and BF9343_1927-26 the names *bti1* (*B. fragilis* T6S immunity 1), *bti2a*, and *bti2b*, respectively. Bte1 and Bte2 fully account for the in vitro killing of both *B. thetaiotaomicron* and *B. vulgatus* (Fig. 1 *A* and *C*), because constitutive expression of *bti1* and *bti2ab* in either symbiont conferred complete protection against wild-type *B. fragilis*^{N} (Fig. 3 *D* and *E*); this suggests that the effector repertoire of *B. fragilis*^{N} is encoded within cassettes A and B, although *B. thetaiotaomicron* and *B. vulgatus* could potentially be resistant to other *B. fragilis*^{N} effectors.

T6SS$^+$ *B. fragilis* Strains Target Susceptible Members of Their Species Both in Vitro and in Vivo. Our comparative genomic analysis revealed that several other strains, such as *B. fragilis* 3986 T(B)9 (*B. fragilis*^{TB9}), lack *bte1* and *bte2* yet encode orphan homologs of *bti1* and/or *bti2ab*, either outside of their T6SS locus or in the absence of a T6SS entirely. Indeed, *B. fragilis*^{TB9} is fully resistant to *B. fragilis*^{N} T6S activity in vitro and in vivo (Fig. 4*A*; Fig. S2*A*). Moreover, the *B. fragilis*^{TB9} *bti2ab* homologs protect an otherwise sensitive *B. fragilis*^{N} recipient strain (lacking *tssC* and both E/I pairs) against *B. fragilis*^{N} Bte2 activity, demonstrating that these orphan immunity homologs are functional (Fig. 4*B*).

Like most bacterial species, *B. fragilis* strains can vary by hundreds to thousands of genes whose functions are largely unknown. To investigate whether T6S can determine the ecological balance between strains in vivo in the context of all of these other factors,

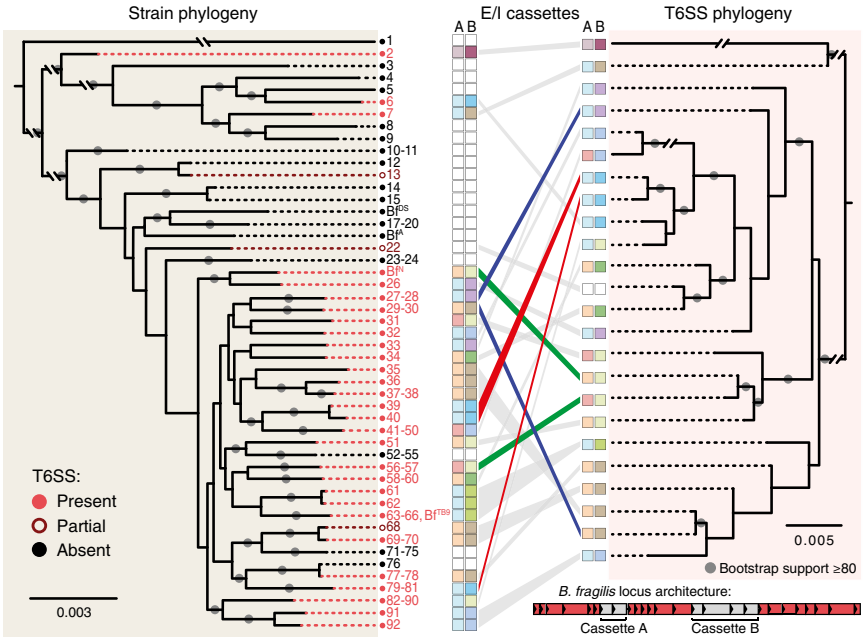

Fig. 2. Comparative genomic analysis of *B. fragilis* strains reveals multiple independent acquisitions of T6SS loci and numerous putative effector/immunity cassettes. Whole-genome phylogeny (*Left*) of all 92 sequenced *B. fragilis* strains (Dataset S1, Table S1) is linked to T6SS locus phylogeny (*Right*) by gray and colored lines. T6SS locus architecture is conserved across T6SS$^+$ *B. fragilis* strains, revealing three conserved, syntenic regions (red shading) and two variable, nonsyntenic regions (gray shading) within each T6SS locus (*Inset*). Putative effector/immunity repertoires of nonsyntenic regions are depicted with colored boxes (Dataset S1, Table S3). The incongruence between the strain and T6SS phylogenetic trees indicate that most *B. fragilis* strains have acquired their T6SS through recent and independent horizontal transfer events. Examples of closely related strains acquiring distinct T6SSs (blue lines), distantly related strains acquiring similar T6SSs (red lines), and similar T6SSs encoding distinct putative E/I pairs (green lines) are shown.

we examined *B. fragilis* ATCC 43859 (*B. fragilis*^{A}), whose genome differs from *B. fragilis*^{N} by 608 genes (including a lack of a T6SS and orphan immunity homologs). As expected, *B. fragilis*^{A} was susceptible to T6S attacks in vitro (Fig. 4*C*). We then gavaged germ-free mice with a mixture of both strains and assessed strain abundances in feces over time. Indeed, *B. fragilis*^{A} was suppressed to less than 5% of the microbiome in the presence of wild-type *B. fragilis*^{N}, but represented nearly half of the microbiome in the presence of the *tssC* control (Fig. 4*D*). Similarly, T6S also determines the ecological balance between the T6SS$^-$ strain *B. fragilis* DS-208 (*B. fragilis*^{DS}) and *B. fragilis*^{N} in vivo (Fig. S2*B*).

Measuring Gut Symbiont T6S-Mediated Killing Rates in Live Animals. Collectively, our data suggest that these contact-based bacterial interactions could play a significant role in shaping gut microbial ecology and highlight strains and species that share an ecological niche. However, the frequency of T6S effector transmission from donor cells to sensitive or resistant recipient cells has never been studied in a natural habitat. The gnotobiotic mouse model, combined with precise genetic manipulation of T6S activity in human symbionts, provides the opportunity to quantify effector transmission rates in the mammalian gut. To this end, we applied a special case of the generalized Lotka–Volterra model (5, 18), which relates experimentally measured changes in the ratio of donor and recipient cells to the abundance of donor cells in the community and the effector transmission rate β:

$$\frac{d}{dt} ln(r) = -\beta D,$$

where D is the concentration of donor cells, r is the ratio of susceptible recipient (S) to donor cells, t is time, and β is a transmission coefficient that quantifies the rate at which donor cells encounter sensitive cells multiplied by the probability that an encounter will lead to successful killing event. This model provides several testable predictions. First, if $\beta = 0$ (no T6SS activity), the ratio between isogenic donor and recipient cells will not change over time. Second, time-series measurements of D and S are sufficient to provide a solution for β.

To test if these populations are in fact stable in the absence of T6S-dependent interactions, we first colonized germ-free mice with *B. fragilis*^{N} *tssC* (representing a D population, where $\beta = 0$) and an isogenic nonimmune derivative lacking the E/I pairs identified above (representing an S population). As expected, the susceptible population remained stable over time, indicating that birth and immigration (by coprophagy) rates are equivalent to death and emigration (loss in feces) rates in this ecosystem at multiple starting ratios of D and S (Fig. 5*A* and Fig. S3*A*). By contrast, the same susceptible population is rapidly and continually depleted when cocolonized with wild-type *B. fragilis*^{N}, at multiple starting ratios of D and S (Fig. 5*A* and Fig. S3*B*). As expected, T6S activity is evident throughout the densely populated large intestine, but not in the small intestine where bacterial colonization densities are orders of magnitude lower (Fig. S3*C*). Consistently, an otherwise susceptible strain is fully protected from T6S-mediated killing in liquid culture where cell-to-cell contact is transient and limited in frequency, and also on solid surfaces if cell contact is blocked by a 0.2-μm filter (Fig. S3 *D* and *E*). Based on over 100 direct measurements of D and S in these animals, a transmission coefficient β of 0.62 ± 0.15 effector transmission events per D cell per day is sufficient to produce the population dynamics observed in vivo (Fig. S4). This transmission rate is equivalent to over 10^9 effector transmission events per minute per gram of colonic contents and is stable over time (Fig. 5*B*).

In humans, *B. fragilis* typically represents 0.1–1% of the microbiome (19); the rest of the community represents a mixture of D, S (other Bacteroides are T6SS$^+$ or T6SS$^-$ and constitute up to 80% of the microbiome), and resistant populations. To determine the impact of a multiphylum community of human gut commensals on the dynamics of D and S *B. fragilis*^{N} populations

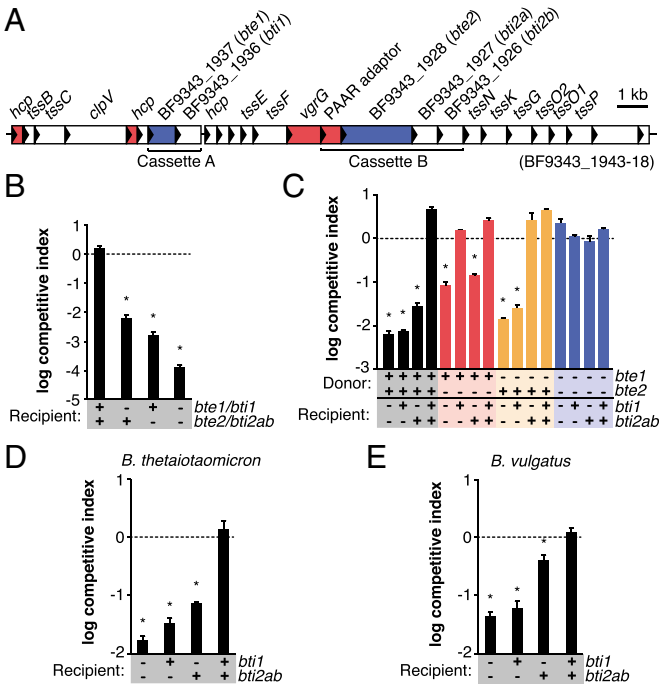

Fig. 3. Identification of T6S-dependent antibacterial effectors and cognate immunity proteins in *B. fragilis*^{N}. (*A*) Secretome profiling reveals two candidate effectors in *B. fragilis*^{N}. Proteins secreted by *B. fragilis*^{N} in a T6S-dependent manner (Dataset S1, Table S4) are mapped onto its T6SS locus (red, known T6SS components; blue, candidate effectors). (*B*) Candidate E/I pairs protect against T6S-mediated killing. *B. fragilis*^{N} donor cells were grown in contact with *B. fragilis*^{N} *tssC* recipient cells carrying deletions of genes encoding the E/I pairs. (*C*) Expression of effector genes causes T6S-mediated killing of recipient cells lacking cognate immunity genes. *B. fragilis*^{N} donor cells were grown in contact with E/I mutant recipient cells expressing immunity genes or carrying an empty vector. (*D* and *E*) *B. thetaiotaomicron* (*D*) and *B. vulgatus* (*E*) are protected from *B. fragilis*^{N} T6S by heterologous expression of immunity genes. Recipient species carry an empty vector or constitutively express *B. fragilis*^{N} immunity genes. In all graphs, $*P < 0.05$. Error bars indicate ± SD ($n = 2$; representative of three independent trials).

across varying abundances, we colonized germ-free mice with either wild-type or *tssC B. fragilis*^{N} (*D* populations), a nonimmune *B. fragilis*^{N} lacking *tssC* and both E/I pairs (*S* population), and a 14-species, T6SS$^-$ human gut community representing three major phyla found in the gut (Dataset S1, Table S5). In these animals, the *D* and *S B. fragilis*^{N} populations initially represent 99% of the microbiome and stabilize over time to ∼1% of the community, approximating *B. fragilis* levels in humans (Fig. 5*C*; Fig. S5). Quantification of each species and the *B. fragilis*^{N} populations over time revealed significant T6S-dependent killing (>10^7 killing events/gram/day) throughout the experiment, even when *B. fragilis*^{N} populations approach 1% of the entire community (Fig. 5*D*). Notably, T6S-dependent killing of the susceptible *S* population decreases over time as the 14-species T6SS$^-$ community increases in relative abundance. To determine whether the observed decrease in T6S-dependent killing could be fully explained by the smaller *D* and *S* populations or also required community protection, we calculated expected killing rates in each time interval, based on the initial measured ratio of *D* and *S* in that interval and the β value determined above. Observed killing rates in the presence of the community were significantly lower than these expected values, and these differences increased in proportion to community abundance (Fig. 5 *C* and *D*), which suggests that the presence of a diverse community enables susceptible individuals to persist despite antagonism by T6S.

Discussion

Genome sequencing of strains isolated from individual human gut microbiomes over time has revealed that individual strains within these communities, particularly Bacteroidetes, can persist for years or decades in humans without significant strain replacement (20). Though metagenomic sequencing highlights broad (i.e., phylum-level) microbiome changes in response to diet, antibiotics, and other factors, the mechanisms that determine community membership at the species- or strain-level are largely unexplored. The human gut and its microbiome is one of the densest known ecosystems, and bacteria that occupy this habitat face stringent competition for dietary and host-derived nutrients localized to food particles or mucus (21); at the same time, they benefit from diffusible vitamins, metabolic by-products, and public goods produced by other species or strains (22, 23). Mechanisms for contact-dependent antagonism, including T6S, could allow cells to minimize local nutritional competition without impacting the fitness of spatially distant bacteria that provide these beneficial compounds. The distribution of T6SS$^+$ strains within (and outside) the Bacteroidetes is not easily predicted due to extensive horizontal gene transfer (Fig. 2). Given that members of this phylum constitute 50–80% of the microbiome in many individuals (19), our results and others (15) suggest that contact-dependent antagonism is a general feature that shapes interbacterial interactions between human gut microbes.

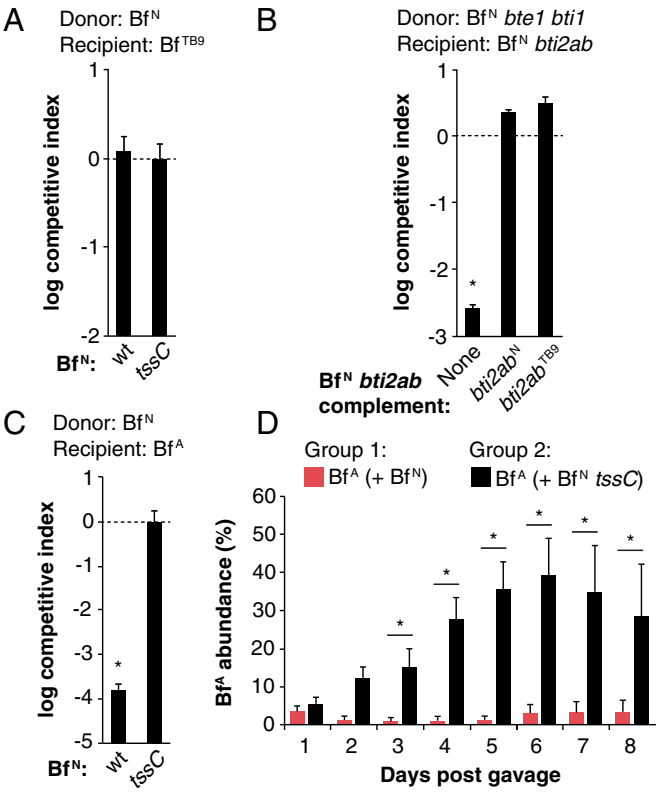

Fig. 4. Interstrain dynamics are determined by T6S antagonism in vitro and in vivo. (*A*) *B. fragilis* 3986 T(B)9 (Bf^{TB9}) is resistant to *B. fragilis*^{N} (Bf^N) T6S in vitro. (*B*) *B. fragilis*^{TB9} T6S immunity homologs are functional. Expression of *B. fragilis*^{N} or *B. fragilis*^{TB9} *bti2ab* homologs confers immunity to a *B. fragilis*^{N} *tssC* mutant lacking its own E/I pairs. (*C* and *D*) Interactions between *B. fragilis*^{N} (Bf^N) and *B. fragilis* ATCC 43859 (Bf^A) are determined by T6S in vitro (*C*) and in vivo (*D*). For all in vitro experiments: $*P < 0.05$. Error bars indicate ± SD ($n = 2$; representative of three independent trials). For *D*, $*P < 0.05$ between recipient populations in each group ($n = 5$ mice per group; representative of two independent trials). Error bars indicate ± SD.

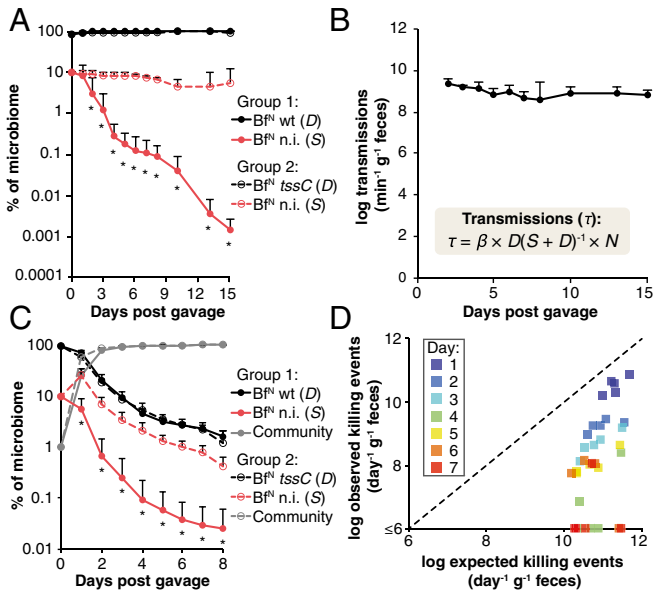

Fig. 5. *B. fragilis* transmits T6S effectors in gnotobiotic mice at rates exceeding 10^9 events per minute per gram of colonic contents. (*A*) Human gut symbiont T6S activity rapidly and continually removes T6S-sensitive cells from the gut. A *B. fragilis*^{N} *tssC* strain lacking both E/I pairs [nonimmune (n.i.); Bf^N n.i.] was introduced as a susceptible (*S*) recipient into germ-free mice with either wild-type *B. fragilis*^{N} (Bf^N WT) or *B. fragilis*^{N} *tssC* (Bf^N *tssC*) as T6S-positive or -negative donor (*D*) strains, respectively, at a 1:10 starting ratio of *S* to *D* populations. $^*P < 0.05$. Error bars indicate ± SD between nonimmune populations in each group ($n = 5$ mice per group; representative of two independent trials). (*B*) Population-level effector transmission rates (τ) exceeding 10^9 events per minute per gram of colonic contents are stable and sufficient to drive the population dynamics observed in Fig. 5*A*. *N* = total population size (*SI Materials and Methods*). Error bars indicate ± SD; see also Fig. S4. (*C*) T6S-mediated killing of a susceptible (*S*) population is modulated by the relative population size of a representative human microbiome. Germ-free mice were colonized with nonimmune *B. fragilis*^{N} (*S*), WT or *tssC B. fragilis*^{N} (*D*), and a 14-species human gut commensal community (Dataset S1, Table S5). $^*P < 0.05$ between nonimmune populations in each group ($n =$ 5 mice per group, representative of two independent trials); error bars indicate ± SD (Fig. S5). (*D*) The presence of the community reduces T6S attacks on susceptible cells in the gut. For each time interval, expected T6S killing events (calculated from the measured *S* to *D* ratios at the beginning of the interval and β quantified from Fig. 5*A*) are compared with observed T6S-dependent killing events in Fig. 5*C*.

As expected from the contact-dependent nature of these interactions, mathematical modeling predicts that the frequency of T6S-mediated killing events reaches a maximum under conditions in which all cells are evenly mixed and donor and recipient cells each constitute half of the community (Fig. S6). Our experiments using defined microbial communities in germ-free mice support these predictions: *B. fragilis*^{N} significantly reduces *B. vulgatus* abundance via T6S when the T6S-positive and -negative cells each represent ~50% of the community (Fig. 1*D*), but this does not occur when the T6S-positive cells represent only 1% (Fig. S5). Similar dynamics may explain the discrepancy between in vitro and in vivo dynamics of T6S-mediated killing of *B. thetaiotaomicron*. Moreover, our model suggests that the decrease in the observed killing rate of *B. fragilis*^{N} in a multispecies community (Fig. 5*D*) does not require an intrinsic reduction in the transmission rate (i.e., decreased β), but instead can be explained by changes in the population dynamics of the microbiome (e.g., altered ratios of donors and recipients over time, uneven mixing of species). Together, these studies highlight the importance of in vivo experiments for understanding the role of contact-mediated interactions between bacteria. Long-term studies could also reveal more subtle or indirect T6S interactions that manifest over one or more host generations.

Identification and genetic manipulation of E/I pairs in *B. fragilis* strains, combined with gnotobiotic animal models in which community composition can be controlled and measured, allows for the calculation of a transmission coefficient ($\beta = 0.62$ per *D* cell per day) for T6S activity in the gut. This calculation represents a lower bound for this activity in vivo for at least three reasons. First, uneven mixing would increase the number of transmission events required to mediate the observed killing rates (Fig. S6*B*). Second, the model assumes that a single effector transmission event into an *S* individual results in the death and subsequent removal of that individual from the population. However, if some proportion of transmission events into *S* cells does not result in the death of the recipient, then those individuals will not be removed from the population, representing transmission events that do not produce an observable change in *S*. Indeed, in vitro studies of the opportunistic proteobacterial pathogen *Pseudomonas aeruginosa* suggest that its T6SS kills recipient cells at rates of ~5% or less per hour of contact (24). Third, our experiments used T6S-negative recipient populations. *P. aeruginosa* cells display an elevated propensity to activate T6S in response to a T6S attack (24, 25). Although this phenomenon has not been investigated in Bacteroides, the *S* strain and 14-species community in these experiments are T6S-negative and would not induce this increased transmission rate that may occur between T6S-positive (*D*) individuals.

From our calculation of effector transmission rates between bacteria, we can predict that humans carrying *B. fragilis* at typical levels (19) host 60–600 billion effector transmission events per day from this species alone. A deeper understanding of the E/I repertoires present among human symbiont strains within an individual microbiome will help to predict the impact of T6S on other community members. Interestingly, our data show that human symbionts can accumulate immunity genes throughout their genomes that protect against T6S effectors that they do not encode, suggesting a selective advantage to maintaining the ability to evade contact-mediated antagonism. Because immunity genes are difficult to recognize by sequence alone (9, 10), many more may exist in the genomes of commensal bacteria. Unlike the immunity genes, *B. fragilis* effectors appear to be encoded in stereotyped positions inside the T6SS locus (Fig. 2). Because numerous human gut Bacteroidetes besides *B. fragilis* carry T6SS loci (11, 12, 15), additional effectors will be readily identifiable in other species. These effectors reveal strategies human gut symbionts themselves have evolved to target other members of this community, and may provide important new approaches for precision microbiome manipulation.

Materials and Methods

Bacterial Culture Conditions. Bacteroides strains (Dataset S1, Table S5) were anaerobically cultured on brain heart infusion (BHI; Becton Dickinson) agar supplemented with 50 μg/mL hemin (Sigma-Aldrich) and 0.5 μg/mL menadione (MP Biomedicals), in liquid tryptone-yeast-glucose (TYG) medium (26), or liquid minimal medium (22). Representative microbiome community members (Dataset S1, Table S5) were grown as previously described (27).

Genetic Techniques. A full list of primers, plasmids, and strains are provided (Dataset S1, Table S5). Genetic manipulation of *B. fragilis* NCTC 9343 was enabled by adapting a counter selectable system originally developed in *B. thetaiotaomicron* (28) for use in *B. fragilis*. Detailed methods can be found in *SI Materials and Methods*.

Comparative Genomics.

Genome phylogenies. The phylogenetic relationship between all 92 available sequenced strains of *B. fragilis* (Dataset S1, Table S1) was assessed by maximum likelihood on sets of ubiquitously distributed genes constituting the core genome, as described in *SI Materials and Methods*.

T6SS identification and phylogenetics. For each genome, T6SS presence/absence was determined by BLASTn (29) search for homologs of the eight core T6SS structural components from *B. fragilis*^{N} that are conserved between Proteobacterial and Bacteroidetes T6SSs (Dataset S1, Table S2) using an E-value

MICROBIOLOGY

cutoff of 0.0001, coverage cutoff of 50%, and identity cutoff of 50%. Detailed methods can be found in *SI Materials and Methods*.

Identification of T6S Effectors by Mass Spectrometry. *B. fragilis*^{N} *tdk* and *B. fragilis*^{N} *tdk tssC* were subcultured from exponential cultures, grown to mid-log phase in minimal medium (22), and pelleted. Proteins in the supernatant were precipitated with trichloroacetic acid, trypsinized, and analyzed by LC-MS/MS as described previously (11). Additional methodological and analytical details can be found in *SI Materials and Methods*.

In Vitro Bacterial Competitions. Strains were grown on BHI agar plates, resuspended in PBS, and adjusted to an OD_{600} of 6.0 for donor strains and 0.6 for recipient strains. Cells were mixed at a 1:1 vol/vol ratio, and 5 μL of each mixture was spotted onto nitrocellulose squares placed on BHI agar plates. After incubation at 37 °C anaerobically for 20–24 h, viable cells were enumerated by serial dilution and plating. Additional methodological and analytical details can be found in *SI Materials and Methods*.

Gnotobiotic Animal Studies. All animal experiments were performed using protocols approved by the Yale University Institutional Animal Care and Use Committee. Male and female germ-free 8- to 12-wk-old Swiss Webster mice were maintained in flexible plastic gnotobiotic isolators with a 12-h light/dark cycle. Mice were individually caged and were provided with standard autoclaved mouse chow (5K67 LabDiet; Purina) ad libitum. Germ-free mice were colonized with bacteria from glycerol stocks by oral gavage. Fecal samples were collected over time and upon sacrificing each mouse, samples were collected along the length of the gut and stored at −80 °C before genomic DNA extraction (27) (*SI Materials and Methods*).

Mathematical Model. Rates of in vivo T6SS activity were determined using a special case of the generalized Lotka–Volterra system commonly used to model microbiome dynamics (5, 18). Details are available in *SI Materials and Methods*.

ACKNOWLEDGMENTS. We thank members of A.L.G.'s laboratory; J. Galán and E. Groisman for helpful discussions; and C. Sears for *B. fragilis*^{TB9} and *B. fragilis*^{DS}. D.R.G. thanks the University of Maryland School of Pharmacy Mass Spectrometry Center (SOP1841-IQB2014). This work was supported NIH Grants GM103574 and GM105456 (to A.L.G.), AI080609 (to J.D.M.), GM101209 and GM108657 (to H.O.), and OD008440 (to J.B.X.); the Pew Scholars Program (A.L.G.); and the Burroughs Wellcome Fund (A.L.G. and J.D.M.). A.G.W. is supported by a fellowship from the Gruber Foundation, and J.C.W. is supported by a fellowship from the Canadian Institutes of Health Research.

1. Arthur JC, et al. (2012) Intestinal inflammation targets cancer-inducing activity of the microbiota. *Science* 338(6103):120–123.
2. Haiser HJ, et al. (2013) Predicting and manipulating cardiac drug inactivation by the human gut bacterium *Eggerthella lenta*. *Science* 341(6143):295–298.
3. Hehemann JH, et al. (2010) Transfer of carbohydrate-active enzymes from marine bacteria to Japanese gut microbiota. *Nature* 464(7290):908–912.
4. Greenblum S, Carr R, Borenstein E (2015) Extensive strain-level copy-number variation across human gut microbiome species. *Cell* 160(4):583–594.
5. Buffie CG, et al. (2015) Precision microbiome reconstitution restores bile acid mediated resistance to *Clostridium difficile*. *Nature* 517(7533):205–208.
6. Kommineni S, et al. (2015) Bacteriocin production augments niche competition by enterococci in the mammalian gastrointestinal tract. *Nature* 526(7575):719–722.
7. Goodman AL, et al. (2009) Identifying genetic determinants needed to establish a human gut symbiont in its habitat. *Cell Host Microbe* 6(3):279–289.
8. Palm NW, et al. (2014) Immunoglobulin A coating identifies colitogenic bacteria in inflammatory bowel disease. *Cell* 158(5):1000–1010.
9. Silverman JM, Brunet YR, Cascales E, Mougous JD (2012) Structure and regulation of the type VI secretion system. *Annu Rev Microbiol* 66:453–472.
10. Russell AB, Peterson SB, Mougous JD (2014) Type VI secretion system effectors: Poisons with a purpose. *Nat Rev Microbiol* 12(2):137–148.
11. Russell AB, et al. (2014) A type VI secretion-related pathway in Bacteroidetes mediates interbacterial antagonism. *Cell Host Microbe* 16(2):227–236.
12. Coyne MJ, Zitomersky NL, McGuire AM, Earl AM, Comstock LE (2014) Evidence of extensive DNA transfer between bacteroidales species within the human gut. *MBio* 5(3):e01305–e01314.
13. Mazmanian SK, Round JL, Kasper DL (2008) A microbial symbiosis factor prevents intestinal inflammatory disease. *Nature* 453(7195):620–625.
14. Karlsson FH, Ussery DW, Nielsen J, Nookaew I (2011) A closer look at bacteroides: Phylogenetic relationship and genomic implications of a life in the human gut. *Microb Ecol* 61(3):473–485.
15. Coyne MJ, Roelofs KG, Comstock LE (2016) Type VI secretion systems of human gut Bacteroidales segregate into three genetic architectures, two of which are contained on mobile genetic elements. *BMC Genomics* 17(1):58.
16. Wilson MM, Anderson DE, Bernstein HD (2015) Analysis of the outer membrane proteome and secretome of Bacteroides fragilis reveals a multiplicity of secretion mechanisms. *PLoS One* 10(2):e0117732.
17. Salomon D, et al. (2014) Marker for type VI secretion system effectors. *Proc Natl Acad Sci USA* 111(25):9271–9276.
18. Coyte KZ, Schluter J, Foster KR (2015) The ecology of the microbiome: Networks, competition, and stability. *Science* 350(6261):663–666.
19. Human Microbiome Project Consortium (2012) Structure, function and diversity of the healthy human microbiome. *Nature* 486(7402):207–214.
20. Faith JJ, et al. (2013) The long-term stability of the human gut microbiota. *Science* 341(6141):1237439.
21. Sonnenburg JL, et al. (2005) Glycan foraging in vivo by an intestine-adapted bacterial symbiont. *Science* 307(5717):1955–1959.
22. Degnan PH, Barry NA, Mok KC, Taga ME, Goodman AL (2014) Human gut microbes use multiple transporters to distinguish vitamin B_{12} analogs and compete in the gut. *Cell Host Microbe* 15(1):47–57.
23. Rakoff-Nahoum S, Coyne MJ, Comstock LE (2014) An ecological network of polysaccharide utilization among human intestinal symbionts. *Curr Biol* 24(1):40–49.
24. LeRoux M, et al. (2012) Quantitative single-cell characterization of bacterial interactions reveals type VI secretion is a double-edged sword. *Proc Natl Acad Sci USA* 109(48):19804–19809.
25. Basler M, Ho BT, Mekalanos JJ (2013) Tit-for-tat: Type VI secretion system counterattack during bacterial cell-cell interactions. *Cell* 152(4):884–894.
26. Holdeman LV, Cato ED, Moore WEC (1977) *Anaerobe Laboratory Manual* (Virginia Polytechnic Inst and State Univ Anaerobe Lab, Blacksburg, VA).
27. Cullen TW, et al. (2015) Antimicrobial peptide resistance mediates resilience of prominent gut commensals during inflammation. *Science* 347(6218):170–175.
28. Koropatkin NM, Martens EC, Gordon JI, Smith TJ (2008) Starch catabolism by a prominent human gut symbiont is directed by the recognition of amylose helices. *Structure* 16(7):1105–1115.
29. Altschul SF, Gish W, Miller W, Myers EW, Lipman DJ (1990) Basic local alignment search tool. *J Mol Biol* 215(3):403–410.
30. Edgar RC (2010) Search and clustering orders of magnitude faster than BLAST. *Bioinformatics* 26(19):2460–2461.
31. Katoh K, Standley DM (2013) MAFFT multiple sequence alignment software version 7: Improvements in performance and usability. *Mol Biol Evol* 30(4):772–780.
32. Stamatakis A (2006) RAxML-VI-HPC: Maximum likelihood-based phylogenetic analyses with thousands of taxa and mixed models. *Bioinformatics* 22(21):2688–2690.
33. Darling AE, Mau B, Perna NT (2010) progressiveMauve: Multiple genome alignment with gene gain, loss and rearrangement. *PLoS One* 5(6):e11147.
34. Huang Y, Niu B, Gao Y, Fu L, Li W (2010) CD-HIT Suite: A web server for clustering and comparing biological sequences. *Bioinformatics* 26(5):680–682.
35. Finn RD, et al. (2014) Pfam: The protein families database. *Nucleic Acids Res* 42(Database issue):D222–D230.
36. Kelley LA, Mezulis S, Yates CM, Wass MN, Sternberg MJ (2015) The Phyre2 web portal for protein modeling, prediction and analysis. *Nat Protoc* 10(6):845–858.
37. Cox J, Mann M (2008) MaxQuant enables high peptide identification rates, individualized p.p.b.-range mass accuracies and proteome-wide protein quantification. *Nat Biotechnol* 26(12):1367–1372.
38. Choi H, Fermin D, Nesvizhskii AI (2008) Significance analysis of spectral count data in label-free shotgun proteomics. *Mol Cell Proteomics* 7(12):2373–2385.
39. Petersen TN, Brunak S, von Heijne G, Nielsen H (2011) SignalP 4.0: Discriminating signal peptides from transmembrane regions. *Nat Methods* 8(10):785–786.
40. Bookout AL, Cummins CL, Mangelsdorf DJ, Pesola JM, Kramer MF (2006) High-throughput real-time quantitative reverse transcription PCR. *Curr Protoc Mol Biol* Chap 15:Unit 15.8.